

Strong Dispersive and Nonlinear Optical Properties of Microresonator-Modified Optical Waveguides

John E. Heebner and Robert W. Boyd

Institute of Optics, University of Rochester, Rochester, New York 14627, USA

ABSTRACT

We describe the dispersive and nonlinear optical properties of microresonator-modified waveguides. While many applications of microresonators demand ultra-high quality factors and as a result impose strict fabrication tolerances, we examine a variety of useful devices that may be constructed using small numbers of only moderately-high Q resonators using the current state of the art in fabrication technology.

Keywords: resonators, microresonators, ring resonators, waveguides, photonics, nonlinear optics, artificial materials

1. INTRODUCTION

Microresonators have attracted much attention in the past decade for use as lasers,^{1,2} add-drop filters,³ sensors,⁴⁻⁶ and dispersion compensators.⁷ Some of these applications are based on glass micro-spheres while others are based on wave-guiding rings or disks fabricated using lithographic and etching techniques. Silica glass micro-spheres can be made with ultra-high quality (Q) factors,⁸⁻¹⁰ but are difficult to fabricate reproducibly and not readily integrated. Integrated microdisk or microring resonators can be fabricated more reproducibly^{11,12} but current fabrication techniques cannot achieve high quality factors. In previous works, theoretical treatments of sequences of microresonators coupled to ordinary waveguides revealed that such microresonator-modified waveguides offer great potential for slowing, dispersing, and intensifying light pulses with promising implications for linear and nonlinear photonics.^{13,14} While fabrication advances have been steadily reducing attenuation losses, small intra-cavity losses are always present and accumulate rapidly in proportion to both resonator Q and the number of resonators forming a device. In this article, we examine what useful devices might be constructed from small numbers of moderately-high Q resonators.

2. FUNDAMENTALS

By situating microdisk or microring resonators near an ordinary waveguide, the dispersion relation governing pulse propagation properties may be modified in a variety of desirable ways. The resulting side-coupled integrated spaced-sequence of resonators (SCISSOR) is depicted in figure 1. In this geometry, the microresonators are evanescently coupled to the waveguide in a manner that, apart from internal attenuation, allow unit amplitude transmission at all frequencies. Because of this property, resonators coupled in this manner are often called all-pass filters. Each spectral component of a waveform interacts with each resonator and leaves the resonator in the same forward direction. While the spectral amplitude is unaffected, the interaction with the resonators results in periodic build-up and group delay spectra with peaks occurring at each of the resonant frequencies ($\omega_m = mc/nR$).

Spectral components near each resonance spend more time circulating within the resonators where they are coherently built-up to a higher intensity. The coherently built-up intensity circulating in the resonators, I_j peaks at each resonance according to,

$$\mathcal{B}_j = \frac{I_j}{I_0} = \frac{1 - r_j^2}{1 - 2r_j \cos \phi_j + r_j^2}, \quad (1)$$

Further author information: (Send correspondence to John E. Heebner)

J.E.H.: E-mail: heebner@optics.rochester.edu, Telephone: 1 585 275 5030

R.W.B.: E-mail: boyd@optics.rochester.edu, Telephone: 1 585 275 2329

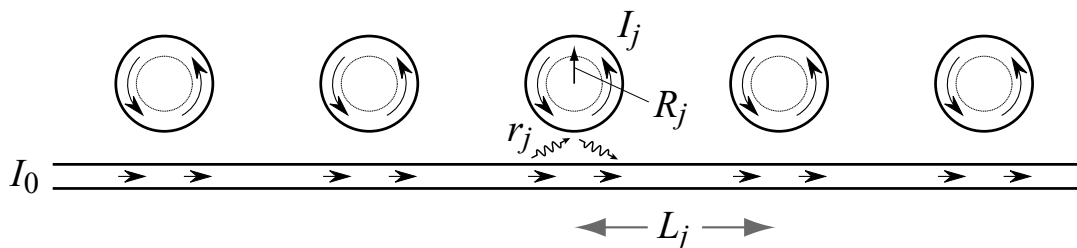


Figure 1. A side-coupled integrated spaced-sequence of resonators (SCISSOR)

where r_j are the lumped coupling parameters and ϕ_j are the normalized detunings ($\phi_j = n\omega 2\pi R_j/c$). For negligible attenuation, the finesse of each coupled resonator is completely defined by the coupling parameter as $\mathcal{F} = \pi/(1 - r)$ and is a measure of the peak build-up ($2\mathcal{F}/\pi$). The distributed group delays can result in a greatly reduced group velocity. Consequently, the slope of the dispersion relation (k_{eff} vs. ω) is steepened near each resonance. The dispersion relation for a SCISSOR is obtained by adding to the propagation constant of the waveguide the distributed phase shifts imparted by the resonators,

$$k_{\text{eff}} = \frac{n\omega}{c} + \sum \frac{\Phi_j}{L_j}. \quad (2)$$

The phase shift imparted by the j th resonator is¹⁵

$$\Phi_j = \pi + \phi_j + 2 \arctan \left(\frac{r_j \sin \phi_j}{1 - r_j \cos \phi_j} \right). \quad (3)$$

Careful choice of the resonator radii, R_j and coupling strengths can lead to a high level of control over the shape of the dispersion relation.

The group index is a convenient measure of the light-slowing properties of a SCISSOR and is obtained from the frequency derivative of the propagation constant,

$$n_g = c \frac{dk_{\text{eff}}}{d\omega} = n_{g0} + c \sum \frac{1}{L_j} \frac{d\Phi_j}{d\phi_j} \frac{d\phi_j}{d\omega}. \quad (4)$$

Written in this manner, the resonator contribution manifests itself as the group delay for a single pass around a resonator circumference, ($d\phi_j/d\omega$), normalized by the retardation time, (L_j/c), and enhanced by the factor $d\Phi_j/d\phi_j$. This factor, known as the phase sensitivity, peaks at a value of $2\mathcal{F}/\pi$ as in the case of the build-up at each resonance.

Figure 2 displays the intensity build-up, dispersion relation, and group index for a SCISSOR. The build-up of intensity and enhancement of group delay are inextricably linked by conservation laws to proportional reductions in other desirable properties - most notably bandwidth. In the case of a Fabry-Perot resonator, the bandwidth is defined by the width of a transmission window which filters periodic bands of frequencies from the reflection spectrum, diverting these bands to the transmission spectrum. In an all-pass resonator, all frequencies are transmitted with equal amplitude but with increased group delay and circulating intensity only across periodic bands of frequencies. These bands, centered at the resonance frequencies possess a full width half maximum (FWHM) detuning bandwidth of $2\pi/\mathcal{F}$ radians. Within this bandwidth, the phase shift imparted by each resonator varies rapidly across π radians. Outside of this interval the rapid variation in phase saturates and becomes clamped on the low and high frequency sides for a total phase shift difference of 2π radians between successive resonances. The saturation in phase leads to strongly dispersive effects both in the linear and nonlinear propagation characteristics. The lowest order dispersive effects are maximized slightly off resonance. The finite variation in phase between two resonance frequencies (across one free-spectral

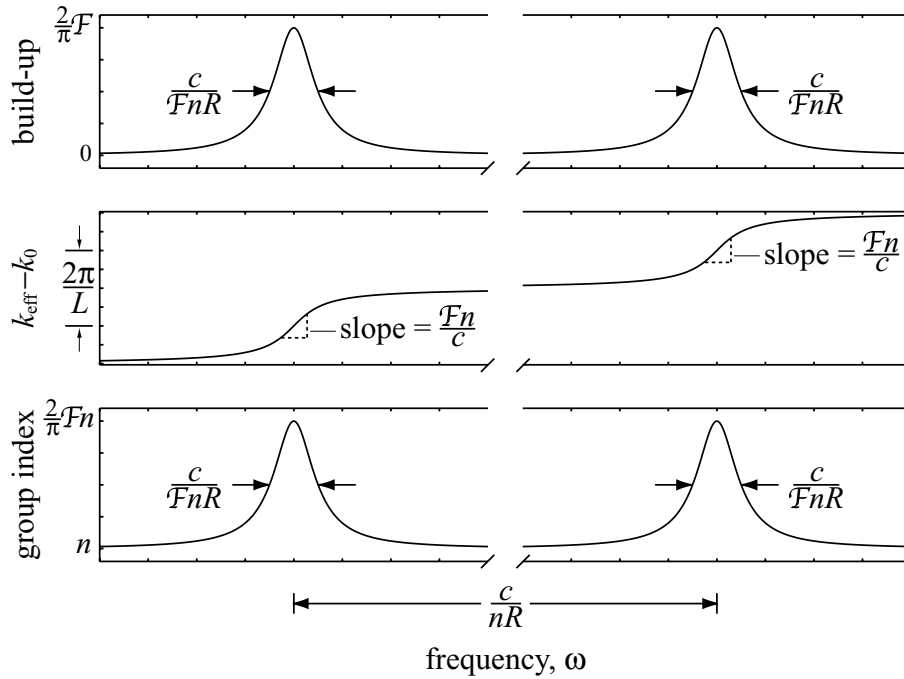


Figure 2. The intensity build-up, propagation constant (or dispersion relation), and group index near two resonances of a SCISSOR. The resonators are assumed to be spaced apart by 2 diameters.

range) is a general property of structural resonances and is independent of the resonator finesse. This property places fundamental limitations on the effectiveness of microresonator-based devices which operate as delay lines, dispersive devices, and nonlinear switches. In the section that follows we demonstrate what useful devices might be constructed while pushing the envelope of these fundamental limitations. Additionally, we will show that the phase-saturating property can be put to use in the form of an optical power limiter.

3. APPLICATIONS

We examine four potential applications of microresonators which do not require an ultra-high finesse or quality factor. For simplicity, in each of these designs incorporating multiple resonators, we assume that all of the resonators possess the same coupling parameters and radii. We consider a tunable optical delay line, an all-optical switch, a pulse compressor, and an optical limiter.

3.1. TUNABLE OPTICAL DELAY LINE

Because the group delay can be controlled by detuning resonators thermally or electro-optically, tunable optical delay lines¹⁶ may be constructed from microresonators. The net group delay, T_D in a SCISSOR increases linearly with the number of resonators,

$$T_D = N \frac{d\Phi}{d\omega}. \quad (5)$$

The net group delay is inversely proportional to the average group velocity which can be minimized by coupling the resonators in a manner that yields the maximum possible finesse. Under this condition, however, the bandwidth may be severely restricted. For example, reducing the group velocity in a SCISSOR by 6 orders of magnitude results in a bandwidth of less than 10 MHz for 10 μm diameter resonators. As a result, designing a SCISSOR for the minimum attainable group velocity (in practice limited by attenuation) is not desirable. The fractional group delay, defined as the group delay normalized to one pulsewidth T_P is a convenient figure of merit characterizing a resonator-based delay line. A fractional group delay near unity corresponds to a delay by

one pulsewidth. This is the greatest delay that can be achieved in a single resonator without the introduction of higher-order dispersive effects. These higher-order dispersive effects result from frequency content in the spectral wings experiencing a lower delay. On resonance, third-order dispersion imposes a pulse distorting phase error which scales as

$$\Phi_{err} = N \frac{1}{6} \frac{d^3 \Phi}{d\omega^3} \Delta\omega^3, \quad (6)$$

where $\Delta\omega$ is the pulse half-bandwidth. Fractional group delays greater than unity can be obtained by use of more resonators. However, dispersive effects accumulate and eventually severely distort pulses. For a desired net fractional delay, these phase errors might be reduced by relaxing the fractional delay per resonator and increasing the number of resonators. Alternatively, the phase errors might be corrected by some means of dispersion compensation, thereby increasing the system complexity. In principle, there is an advantage to using nonlinear soliton propagation in a SCISSOR. Soliton propagation is supported in a SCISSOR resulting from a balance between enhanced self-phase modulation and anomalous (negative) resonator-induced dispersion.¹³ Dispersion of negative sign can be obtained by tuning slightly above resonance. Pulse propagation in this regime is more robust and only affected by still higher-order dispersive effects (fourth-order). In practice, nonlinear phenomena will add other complexities, but it is nevertheless worth examining what is gained.

Figure 3 displays the results of a simulation of a tunable delay line based on a SCISSOR. Eight bits of a 160 Gb/s pulse train show in (a) are delayed by 1 and 4 bit-slots. For simplicity, the delay associated with propagation in the side-coupling waveguide is removed. In (b) six resonators are sufficient to delay the pulse-train by a single bit-slot while suffering minor third-order phase distortion. In (c) a four bit-slot delay is achieved via the use of 26 resonators but the pulses emerge greatly dispersed. By tuning the resonator and pulse energy to parameters near the SCISSOR soliton for the structure, pulse fidelity can be improved as demonstrated in (d). Note that a delay of 4 bit-slots corresponds to a fractional delay of 12 for the duty cycle of 1/3 employed. When the same pulse train is sent through the SCISSOR tuned far away from resonance, either for weak or strong pulses, the pulse train is indistinguishable from that in (a). Thus the delay accumulated in the off-resonance state where pulses effectively bypass the resonators is negligible. This demonstrates the possibility for tunable delay. Most importantly, this simulation demonstrates that a unit fractional delay does not require an ultra-high finesse, but rather is achieved when the pulse bandwidth is of the order of the resonator bandwidth. In order that sequences of resonators forming the SCISSOR overlap in their delay bandwidths, their effective optical circumferences must be made reproducibly to within the wavelength divided by the finesse. If the reproducibility does not conform to this standard, a Doppler-like broadening of the Lorentzian resonance linewidths will result in lowered group delay and broader bandwidth.

3.2. NONLINEAR OPTICAL SWITCH

Owing to an increased interaction length (related to the increase in phase sensitivity) and coherent build-up of circulating intensity, all-pass microresonators can dramatically enhance accumulated nonlinear phase shifts. As described earlier, enhanced self-phase modulation can be used to propagate SCISSOR solitons. The enhancement can also be used to construct compact all-optical switches operating with greatly reduced switching thresholds. As with many other optical properties, however, an all-pass resonator enhances nonlinear phase shifts at the cost of imposing a limitation on the bandwidth over which this enhancement takes place. We have shown in a previous letter¹⁵ that while this conservation law holds for the linear optical properties, it may be circumvented for some nonlinear optical properties, in particular self-phase modulation.

The bandwidth of a resonator is primarily governed by its size and finesse:

$$\Delta\nu = \nu_0/Q = c/(n2\pi RF). \quad (7)$$

For an all-pass resonator with an intensity-dependent refractive index, this bandwidth corresponds to the frequency interval over which the phase varies sensitively and in a nearly linear manner over π radians. Outside this interval the sensitivity rapidly diminishes. A nonlinear phase shift of π radians is sufficient to achieve a switch in an interferometric configuration. The threshold power required to achieve a π radian nonlinear phase shift is reduced in quadratic proportion to the finesse¹⁵:

$$P_\pi = \frac{\pi\lambda A_{\text{eff}}}{16\mathcal{F}^2 n_2 R}, \quad (8)$$

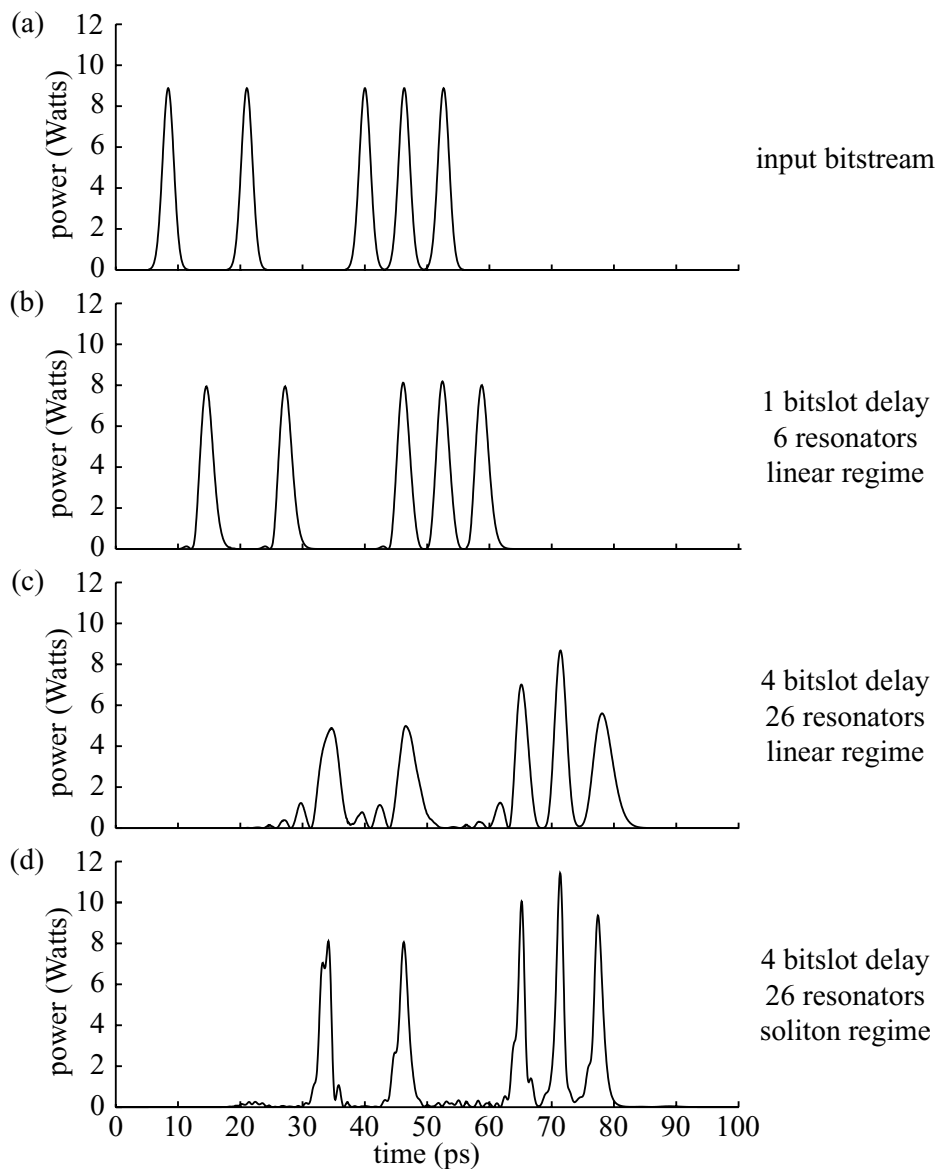


Figure 3. A microresonator-based tunable delay line. The input, shown in (a) consists of 8 bits of a 160 Gb/s (duty cycle=1/3) pulse train. In (b) 6 resonators achieve a delay of a single bit-slot with some minor distortion resulting from third-order dispersion. In (c) 26 resonators achieve a delay of 4 bit-slots though with increased distortion. In (d) propagation near parameters associated with a SCISSOR soliton results in noticeably less distortion. In all cases, a finesse of 10π and $4 \mu\text{m}$ diameters are used. The bit sequence is 10100111.

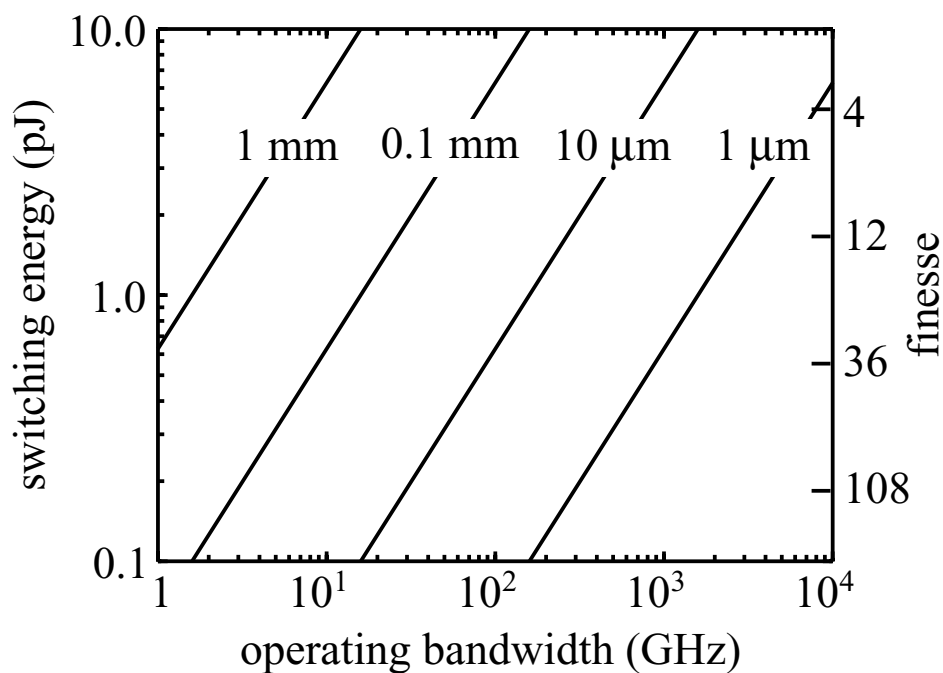


Figure 4. A systems chart displaying the tradeoff between switching energy and bandwidth for single all-pass resonators of varying diameter. The chart assumes high-contrast wave-guiding and a Kerr-based AlGaAs or chalcogenide nonlinearity near $1.55 \mu\text{m}$.

The lowest attainable switching energy is obtained when the pulsewidth is of the order of the cavity lifetime (inverse of the resonator bandwidth). This is easily understood because a longer pulse with the same peak power will carry more energy but not be any more effective at switching. A shorter pulse will not allow the resonator sufficient time to build-up in intensity and thus will experience a weakened nonlinear response in addition to being severely distorted. For a high-contrast dielectric waveguide, the effective area to which the power is confined may be as small as $\lambda^2/8n^2$ where n is the refractive index of the guiding layer. The threshold energy required to achieve a π nonlinear phase shift is accordingly:

$$U_{\pi} = \frac{\lambda^3 \sqrt{\pi^3 \ln(2)}}{64 \mathcal{F} n n_2 c}. \quad (9)$$

In order to reduce the parameter space we make some parameter choices ($n = 3, n_2 = 1.5 \cdot 10^{-17} \text{ m}^2/\text{W}$) corresponding to AlGaAs or chalcogenide^{17,18} glass waveguides operating near $1.55 \mu\text{m}$. Using these material parameters, figure 4 displays a systems chart displaying the tradeoff between switching energy and bandwidth for resonators of varying diameter. It is of technological interest to note that ultra-fast optical switching is possible in a single compact microresonator with a 1 picosecond, 1 picojoule pulse.

Enhanced, all-optical switching has been demonstrated for 30 ps pulses in nonlinear GaAs add-drop filters^{19,20} where the excitation photon energy was above the half-band-gap. In this regime, a strong refractive nonlinearity results from electronic carriers excited into the conduction band and the switching time is limited by electron-hole recombination times. Still faster switching times are feasible by raising the half-band-gap²¹ above the photon energy and optimizing the resonator coupling and radius.

The placement of a nonlinear all-pass resonator within one arm of an interferometer, for example a Mach-Zehnder, allows for the conversion of phase modulation into amplitude modulation which can serve as a basis for an all-optical nonlinear switch. One might ask why one would want to use this indirect method of implementing a microresonator as an amplitude switching device when a nonlinear add-drop filter (resonator coupled to two

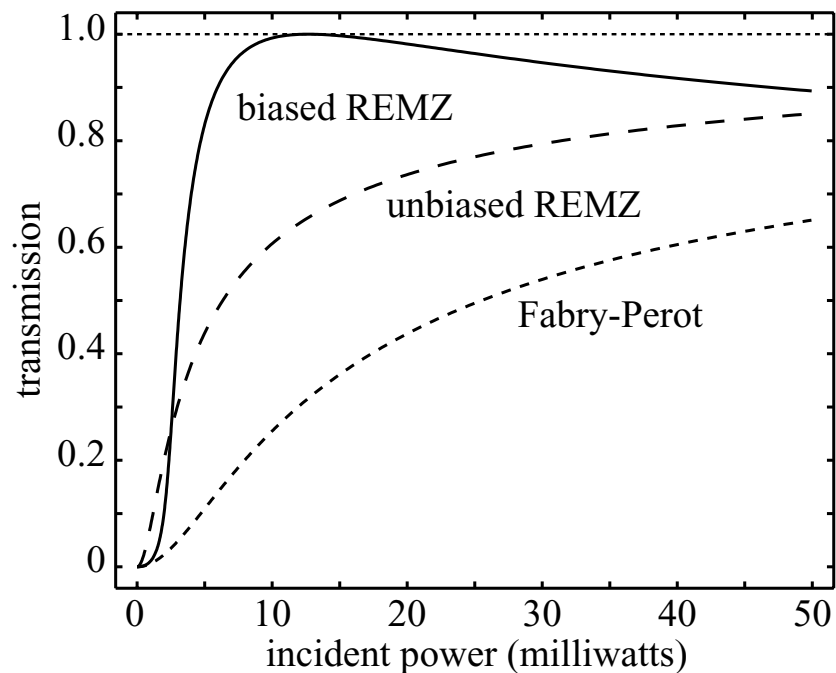


Figure 5. A comparison of the nonlinear switching characteristics of an add-drop filter (Fabry-Perot), an unbiased, and a properly-biased resonator-enhanced Mach-Zehnder (REMZ) interferometer.

waveguides) accomplishes the same task in a more direct manner. The properties of an add-drop filter are analogous to that of a traditional Fabry-Perot interferometer which offers light the choice of two output ports and can display nonlinear amplitude switching between them. A careful examination of a nonlinear add-drop filter as a switching device; however, reveals a fundamental limitation. The switching curve cannot be made to perform a complete switch within the phase sensitive region near resonance. This is because the center of the phase sensitive region (at a resonance frequency) directly coincides with a minimum or maximum of transmission. Only half of the sensitive region is usable as a switch, the other half being wasted. It would be advantageous to shift the peak in phase sensitivity away from the transmission minimum such that it coincides with the linear portion of the transmission curve. However, there is simply no way to accomplish this in an add-drop filter or Fabry-Perot. The missing degree of freedom which can provide this capability can be found in a device formed from a nonlinear all-pass resonator coupled to one arm of an interferometer such as in a resonator-enhanced Mach-Zehnder (REMZ) interferometer. A REMZ can be used to independently set the peaks of nonlinear phase sensitivity and transmission allowing for optimized switching characteristics. Figure 5 compares the switching characteristics for an add-drop filter, an unbiased REMZ and a properly-biased REMZ. For the add-drop filter, the build-up and finesse are each lower by a factor of four in comparison with an all-pass resonator with the same coupling strength. In a REMZ, however, only half of the power enters the arm containing the resonator and its phase contributes in a manner that another factor of two is lost. Still, this results in a net improvement in switching threshold by a factor of four which can be seen by comparing the curves in the figure. It might be argued that this is not a valid analysis since the finesse is not maintained equal in the comparison. When the finesse is maintained equal, the curves are in fact equivalent. More significant, however, is the improvement in the shape of the switching curve when the REMZ is properly biased. Proper biasing is achieved by tuning the peak of the nonlinear phase sensitivity to the 50% transmission operating point of the unloaded Mach-Zehnder.

In this section, we analyzed the tradeoffs associated with the construction of ultrafast, compact all-optical switching devices based on single moderately-high finesse resonators. Improvements over the classical nonlinear Fabry-Perot can be achieved by implementing a more general class of resonator-enhanced interferometer.

3.3. NONLINEAR OPTICAL PULSE COMPRESSOR

We next examine more complicated interaction of structural dispersion and enhanced self-phase modulation in a SCISSOR structure. The soliton order N_S , proportional to the injected amplitude, is a convenient measure of the relative strengths of the two processes. If the relative strengths of the processes are balanced ($N_S = 1$), it was previously shown that soliton-like pulses may be propagated.¹⁴ If however, the nonlinearity dominates the dispersion ($N_S > 1$), pulse compression can result. Because the enhanced nonlinearity and induced dispersion are each proportional to the finesse squared,¹⁴ the soliton order for a SCISSOR can be set by simply choosing the ratio of the pulsewidth to the ring transit time (T_R),

$$N_S = \frac{8\pi}{27^{1/4}} \sqrt{\frac{n_2 I_0 R T_P}{\lambda T_R}} \quad (10)$$

Figure 6 demonstrates the result of a simulation in which a 5 ps Fourier transform-limited pulse is injected into a 10 resonator SCISSOR tuned above resonance at the peak of anomalous dispersion. Here, higher-order breathing solitons are unstable due to the existence of higher-order dispersive effects. As a result, the injected $N_S = 5$ pulse fractures into multiple solitons of differing amplitudes along with some dispersing waves. Due to an intensity-dependent group velocity, the solitons walk away from each other linearly in time. Here, the soliton with the largest amplitude emerges compressed by a factor of approximately five.

The process of temporal imaging is closely related to pulse compression. With temporal imaging,²² intra-pulse structure can be preserved and magnified (or demagnified). An imaging condition must be satisfied in a setup which consists of an initial dispersive segment, an imposed quadratic phase and final dispersive segment of opposite sign to that of the initial. Owing to the large dispersive and nonlinear properties of microresonators, temporal imagers might be fabricated on an integrated photonic chip. Each of the three sections might be composed of differently tuned SCISSOR elements. Sign selection of the dispersive segments is easily accomplished in SCISSORs tuned below (normally dispersive) or above (anomalously dispersive) resonances. The quadratic phase chirp providing the temporal lensing may be accomplished by cross-phase modulation imposed chirp enhanced in a resonant SCISSOR.

3.4. NONLINEAR OPTICAL POWER LIMITER

Injected light initially tuned near the resonance of an all-pass resonator can pull itself off resonance via nonlinear refractive index changes. This leads to a saturation of the enhanced nonlinear phase shift with respect to the injected intensity at high circulating intensities. By incorporating the resonator inside a Mach-Zehnder interferometer, the saturating nonlinear phase shift at high powers can be converted into a clamping of *transmission*. A more carefully designed device can provide a clamping of optical *power*. Figure 7 displays the results of a REMZ-based power limiter which provides near unit transmission until it is lowered systematically such that the power is clamped at 1 watt. Here the normal π radian power for an equivalent length of waveguide is 1 kW. The other port of the REMZ in fact mimics the properties of a saturable absorber where high power levels are transmitted with low loss while low power levels are attenuated.

4. CONCLUSIONS

The construction of high-finesse resonator-based photonic devices is limited in practice by scattering losses and difficulties associated with reproducibility. The severity of these problems may be relaxed if the resonators are of only moderately-high finesse. In this article, we have examined what useful devices might be constructed in this regime. We find that while high-resolution add-drop filters and sensors typically require ultra-high finesse resonators, many other devices do not. Through simulations we analyzed the operation of a tunable optical delay line, an all-optical switch, a pulse compressor, and an optical limiter. While fabrication of high index contrast microresonators remains difficult, we believe these can be implemented using current fabrication technology.

ACKNOWLEDGMENTS

We would like to acknowledge Nick Lepeshkin, Aaron Schweinsberg, Richart Slusher, John Sipe, Philip Chak, and Deborah Jackson.

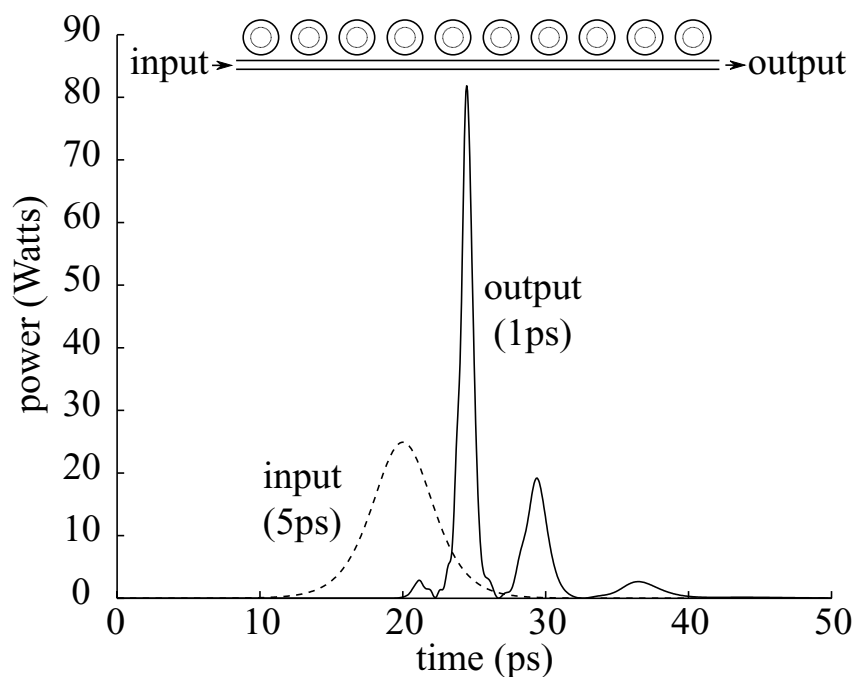


Figure 6. A highly compact microresonator-based 5X pulse compressor. A 25 Watt transform-limited input pulse ($N_S = 5$) of 5 ps width is compressed to 1 ps. In the process, some energy is shed in the form of other non-dispersing pulses which walk away from each other linearly in time owing to an intensity-dependent group velocity. These extra pulses might be eliminated through use of a saturable absorbing material which may even be microresonator-based. Here, 10 AlGaAs or chalcogenide-based microresonators of $10 \mu\text{m}$ diameter form a SCISSOR. The resonators possess a finesse of 5π , coherent intensity build-up of 10, and nonlinear enhancement of 100.

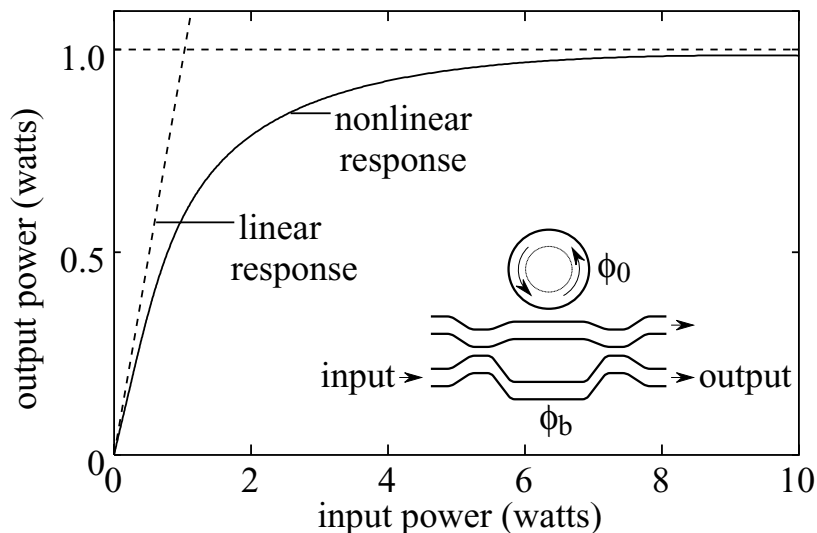


Figure 7. A resonator enhanced Mach-Zehnder (REMZ) interferometer can be implemented as a power limiter. Here, the output power closely follows the input power for power levels much less than 1 W. For higher input power levels, the output power is clamped below 1 W while excess power is diverted to the other output port. The threshold power to achieve a nonlinear phase shift of π radians in a single pass through the resonator is 1 kW, the coupling coefficient is $r = .95$, single pass transmission is 98%, resonator detuning is $\phi_0 = -0.0065\pi$, and the Mach-Zehnder bias is $\phi_b = -0.854\pi$.

REFERENCES

1. S. L. McCall, A. F. J. Levi, R. E. Slusher, S. J. Pearton, and R. A. Logan, "Whispering-gallery mode microdisk lasers," *Appl. Phys. Lett.* **60**, p. 289, 1992.
2. S. M. Spillane, T. J. Kippenberg, and K. J. Vahala, "Ultralow-threshold raman laser using a spherical dielectric microcavity," *Nature* **415**, p. 621, 2002.
3. B. E. Little, S. T. Chu, H. A. Haus, J. Foresi, and J.-P. Laine, "Microring resonator channel dropping filters," *J. Light. Technol.* **15**, p. 998, 1997.
4. A. Serpengzel, S. Arnold, and G. Griffel, "Excitation of resonances of microspheres on an optical fiber," *Opt. Lett.* **20**, p. 654, 1995.
5. S. Blair and Y. Chen, "Resonant-enhanced evanescent-wave fluorescence biosensing with cylindrical optical cavities," *Appl. Opt.* **40**, p. 570, 2001.
6. J. E. Heebner and R. W. Boyd, "Sensitive disk resonator photonic biosensor," *Appl. Opt.* **40**, p. 5742, 2001.
7. C. K. Madsen and G. Lenz, "Optical all-pass filters for phase response design with applications for dispersion compensation," *IEEE Phot. Tech. Lett.* **10**, p. 994, 1998.
8. M. L. Gorodetsky, A. A. Savchenkov, and V. S. Ilchenko, "Ultimate q of optical microsphere resonators," *Opt. Lett.* **21**, p. 453, 1996.
9. S. Schiller and R. L. Byer, "High-resolution spectroscopy of whispering gallery modes in large dielectric spheres," *Opt. Lett.* **16**, p. 1138, 1991.
10. L. Collot and V. Lefevre-Seguin, "Very high-q whispering-gallery mode resonances observed on fused silica microspheres," *Europhys. Lett.* **23**, p. 327, 1993.
11. D. Rafizadeh, J. P. Zhang, S. C. Hagness, A. Taflove, K. A. Stair, S. T. Ho, and R. C. Tiberio, "Waveguide-coupled algaas/gaas microcavity ring and disk resonators with high finesse and 21.6 nm free-spectral range," *Opt. Lett.* **22**, p. 1244, 1997.
12. K. Djordjev, S. Choi, S. Choi, and P. D. Dapkus, "High-q vertically coupled inp microdisk resonators," *IEEE Phot. Tech. Lett.* **14**, p. 331, 2002.
13. J. E. Heebner, R. W. Boyd, and Q. Park, "Slow light, induced dispersion, enhanced nonlinearity, and optical solitons in a resonator-array waveguide," *Phys. Rev. E* **65**, p. 036619, 2002.
14. J. E. Heebner, R. W. Boyd, and Q. Park, "Scissor solitons and other propagation effects in microresonator modified waveguides," *J. Opt. Soc. Am. B* **19**, p. 722, 2002.
15. J. E. Heebner and R. W. Boyd, "Enhanced all-optical switching by use of a nonlinear fiber ring resonator," *Opt. Lett.* **24**, p. 847, 1999.
16. G. Lenz, B. J. Eggleton, C. K. Madsen, and R. E. Slusher, "Optical delay lines based on optical filters," *IEEE J. Quant. Elec.* **37**, p. 525, 2001.
17. S. Spalter, H. Y. Wang, J. Zimmermann, G. Lenz, T. Katsufuji, S. W. Cheong, and R. E. Slusher, "Strong self-phase modulation in planar chalcogenide glass waveguides," *Opt. Lett.* **27**, p. 363, 2002.
18. J. M. Harbold, F. O. Ilday, F. W. Wise, J. S. Sanghera, V. Q. Nguyen, L. B. Shaw, and I. D. Aggarwal, "Highly nonlinear as-s-se glasses for all-optical switching," *Opt. Lett.* **27**, p. 119, 2002.
19. V. Van, T. A. Ibrahim, K. Ritter, P. P. Absil, F. G. Johnson, R. Grover, J. Goldhar, and P.-T. Ho, "All-optical nonlinear switching in gaas-algaas microring resonators," *IEEE Phot. Tech. Lett.* **14**, p. 74, 2002.
20. T. A. Ibrahim, V. Van, and P.-T. Ho, "All-optical time-division demultiplexing and spatial pulse routing with a gaas/algaas microring resonator," *Opt. Lett.* **27**, p. 803, 2002.
21. V. Mizrahi, K. W. DeLong, G. I. Stegeman, M. A. Saifi, and M. J. Andrejco, "Two photon absorption as a limitation to all-optical switching," *Opt. Lett.* **14**, p. 1140, 1989.
22. C. V. Bennett and B. H. Kolner, "Upconversion time microscope demonstrating 103x magnification of femtosecond waveforms," *Opt. Lett.* **24**, p. 783, 1999.